Culture of human mesenchymal stem cells on microcarriers in a 5 L stirred-tank bioreactor

Qasim A. Rafiq[1], Kathryn M. Brosnan[1], Karen Coopman[1], Alvin W. Nienow[1,2] and Christopher J. Hewitt[1*]

[1]*Centre for Biological Engineering, Department of Chemical Engineering, Loughborough University, Leicestershire, LE11 3TU, United Kingdom.*

[2]*School of Chemical Engineering, University of Birmingham, Edgbaston, Birmingham, B15 2TT, United Kingdom.*

**Author for correspondence. (Fax: +44-1509 222506; E-mail: c.j.hewitt@lboro.ac.uk)*

Keywords: human mesenchymal stem cells; regenerative medicine bioprocessing; microcarriers; bioreactor; spinner flask; metabolite profiles; proliferation

Abstract

For the first time, fully functional human mesenchymal stem cells (hMSCs) have been cultured at the litre-scale on microcarriers in a stirred-tank 5 l bioreactor, (2.5 l working volume) and were harvested via a potentially scalable detachment protocol that allowed for the successful detachment of hMSCs from the cell-microcarrier suspension. Over 12 days, the dissolved O_2 concentration was $\succ$ 45 % of saturation and the pH between 7.2 and 6.7 giving a maximum cell density in the 5 l bioreactor of 1.7 $\times$ 10^5 cells/ml; this represents $\succ$sixfold expansion of the hMSCs, equivalent to that achievable from 65 fully-confluent T-175 flasks. During this time, the average specific O_2 uptake of the cells in the 5 l bioreactor was 8.1 fmol/cell h and, in all cases, the 5 l bioreactors outperformed the equivalent 100 ml spinner-flasks run in parallel with respect to cell yields and growth rates. In addition, yield coefficients, specific growth rates and doubling times were calculated for all systems. Neither the upstream nor downstream bioprocessing unit operations had a discernible effect on cell quality with the harvested cells retaining their immunophenotypic markers, key morphological features and differentiation capacity.

Introduction

Regenerative medicine, of which cell-based therapies will play a significant role, has the potential to revolutionise the healthcare industry and replicate the success of the human therapeutic protein industry, which is currently valued at approximately UK£30 billion (Want et al. 2012). For this to be achieved however, manufacturing platforms must be developed for the reproducible production of clinically-relevant numbers of anchorage-dependent cells. Until now, anchorage-dependent stem cells, including human mesenchymal stem cells (hMSCs), have mainly been cultured as a monolayer on two-dimensional platforms such as tissue culture-treated plastic, including cell factories and roller bottles. Although such methods are commonly used and considered reliable, they pose significant limitations with respect to scale-up. For clinical indications which will require lot sizes of billions, if not trillions of cells (Rowley et al. 2012), it is clear that these traditional two-dimensional expansion methods are unsuitable. As such, other methods are being investigated (Want et al. 2012; Rowley et al. 2012) and a promising alternative is the usage of microcarrier-based systems in bioreactors.

Microcarrier technology not only provides a significantly larger surface area per unit volume of bioreactor (Nienow 2006) compared to T-flask culture, but also combines the potential ease of scalability, flexible modes of operation, process monitoring and control capability associated with bioreactor cultures that makes bioreactor culture so widespread in the biopharmaceutical industry. Microcarrier culture is commonly used as a large-scale expansion technique for the culture of adherent cells in vaccine production and was first described by van Wezel (1967) who used positively charged DEAE-Sephadex beads to culture rabbit embryonic skin cells and human embryonic lung cells (van Wezel 1967). However, in vaccine development, the product of interest

is usually an attenuated/killed virus, with little or no attention paid to the cell during downstream processing. For cell-based therapies, the basis of the product of interest is the cell itself, and therefore the focus is not only on cell expansion but also cell quality after harvesting from the bioreactor. A number of challenges in adapting this technology for use in the large-scale expansion of anchorage-dependent stem cells such as hMSCs therefore remain.

Human MSCs are a key human stem cell candidate for large-scale culture due to their multipotency, relative ease of isolation, self-renewal and proliferative capacity, therapeutic efficacy and immunosuppressive properties (Pittenger et al. 1999; Jackson et al. 2007). Human MSCs have been defined by the International Society for Cellular Therapy as being plastic adherent, positive for the expression of CD73, CD90 and CD105 specific surface antigens, negative for the expression of CD14, CD19, CD34, CD45 and HLA-DR specific surface antigens, and possessing the capacity to differentiate towards the chondrogenic, adipogenic and osteogenic lineages *in vitro* (Dominici et al. 2006). With over 120 clinical trials taking place involving the use of hMSCs (Trounson et al. 2011), there is now a clear need for the development of platform technologies for their large-scale culture which would yield them in sufficient quantity and quality. Studies have taken place investigating the culture of hMSCs on microcarriers with a range of commercially available microcarriers being used including Cytodex-1 (Frauenschuh et al. 2007; Schop et al. 2008), Cytodex-3 (Hewitt et al. 2011), Cultispher-S (Eibes et al. 2010), Cultispher-G (Sun et al. 2010) and SoloHill Plastic P102-L (Dos Santos et al. 2011). However in all the aforementioned studies, the largest volume used was no more than 200 mL and it is unclear as to whether samples of

microcarrier suspension greater than 2 mL were harvested. Detachment of cells from the microcarrier surface and subsequent retention of cell quality is equally as important as cell attachment and proliferation given that the product of interest for cell-based therapies is the cells. Therefore it is of paramount importance to consider cell harvesting strategies from the outset so as to ensure a viable, holistic bioprocess.

In this work, hMSCs isolated from bone marrow were cultured in fully controllable 5 L bioreactors at a working volume of 2.5 L for a period of 12 days on plastic microcarriers. These microcarriers were selected based on their suitability for the culture of hMSCs relative to a number of other microcarriers as identified in previous unpublished studies conducted by the authors (data not shown) as well as other groups (Dos Santos et al. 2011), in addition to their amenability for good manufacturing practise (GMP) bioprocesses, given their xeno-free composition. Whilst it would be possible to control the pH and dO_2 levels in the bioreactors, it was decided that this investigation would be used to monitor and identify the change in pH and dO_2 over the course of the culture as there is little work in the literature which identifies the optimal pH and dO_2 levels for microcarrier hMSC culture. Online monitoring of pH and dO_2 is a rarity in hMSC culture (monolayer or microcarrier). Thus being able to shift from an unmonitored to an online monitored process with the possibility of control is a significant step. Cells were also cultured in duplicate 100 mL spinner flasks in parallel to the bioreactors for comparison.

1. Materials and Methods

2.1 hMSC monolayer expansion

Human MSCs were isolated from bone-marrow aspirate donated by Lonza (Lonza, Cologne AG), which had been obtained from a healthy donor after the patient provided informed consent. The local Ethical Committee approved the use of the sample for research. Cells from passage 1 were cryopreserved at a density of 2 x 10^6 cells.mL^{-1} in 2 mL of 0.5% human serum albumin (v/v) (Sigma, Germany), 5 mL of dimethylsulphoxide (Sigma, Germany) and 93 mL of plasmalyte-A (Baxter, Germany). Cells were cultured with Dulbecco's Modified Eagle Medium (DMEM; Lonza, UK) supplemented with 10% (v/v) foetal bovine serum (FBS; Hyclone, Lot# RUF35869) and 2 mM ultraglutamine (Lonza, UK). Cells were grown in monolayer culture at 37^{o}C in T-flasks seeded at an initial density of 5000 cells.cm^{-2} and were placed in a humidified CO_2 controlled incubator which had air supplemented with 5% CO_2. A complete medium exchange was performed after 72 h of culture and cells were passaged at day 6 of culture (the usual time found by us for early-stage passage hMSCs to reach confluency). On passage, the hMSCs were washed with Ca^{2+} and Mg^{2+} free phosphate buffered saline (PBS; Lonza, UK) and then incubated for 4 min with trypsin (0.25%)/EDTA solution (Lonza, UK) to aid cell detachment from the culture plastic. Trypsin was then inactivated by the addition of fresh growth medium equivalent to 3x the volume of the trypsin solution used for cell detachment. The cell suspension was then centrifuged at 220 g for 3 min at room temperature, the supernatant discarded and the remaining pellet re-suspended in an appropriate volume of culture medium. Viable cells were counted and an appropriate number of cells were then re-seeded to a fresh T-

flask. 2 passages were required in order to obtain sufficient cell numbers for seeding of the bioreactors and spinner flasks.

2.2 Bioreactor and spinner flask culture

5 L Biostat B Plus bioreactor (diameter, T = 160 mm) (Sartorius Stedim, UK), equipped with a 3-blade 45°-pitch wide blade impeller (diameter, D =70 mm) and 4 vertical baffles and a dished base were used, each fitted with dissolved oxygen (dO_2), temperature and pH probes (Hamilton, Germany) at a working volume of 2.5 L. The bioreactor was operated throughout the culture period without sparging or headspace flushing with air, though during the exchange of media additional dissolved oxygen entered the bioreactor. pH and dO_2 were measured continuously and the temperature was controlled via a water jacket at 37°C. 100 mL spinner flasks (diameter, T = 60 mm) (BellCo, USA) with a magnetic horizontal stir bar and a vertical paddle (diameter, D = 50 mm) were used in parallel to the bioreactors. One cap on each spinner flask was left loose to allow for gas exchange. Spinner flasks were set up on a Bell-Ennium™ Compact 5 position magnetic stirrer platform (BellCo, USA), maintained in a 37°C, humidified CO_2 controlled incubator which had air supplemented with 5% CO_2. All glass vessels were siliconized using Sigmacote (Sigma, UK) and left overnight prior to autoclaving and rinsing with deionised water. 10,000 cm^2 surface area of solid, non-porous Plastic P-102L microcarriers (Solohill Engineering Inc., US) was used for each bioreactor and prepared in accordance with the manufacturer's specification. Prior to cell inoculation, microcarriers were conditioned with 1 L growth medium for at least 1 h. Cells were seeded at a density of 6000 cells.cm^{-2}, which equates to approximately 5

cells per microcarrier bead. A 50% medium exchange was performed at day 3, and then every 2 days thereafter.

Following inoculation, the culture was static for a period of 18 h, after which the culture was agitated constantly at N_{JS} (the impeller speed at which the microcarriers were just suspended). This speed was selected as it would ensure that all of the cells attached to the microcarrier surface would be available for mass transfer of nutrients to them and metabolites from them. These transfer rates are very insensitive to agitation speed above N_{JS} (Nienow 1997b) but the potential for damage increases rapidly as speed increases (Croughan et al. 1987; Nienow 2006). Thus, N_{JS} as the operating speed is an appropriate choice. N_{JS} was determined visually for the 3-blade 45°-pitch segment impeller and a Rushton turbine impeller with 6 vertical blades. The impellers had the same N_{JS} but the latter has a higher specific energy dissipation rate due to its much higher power number (Ibrahim and Nienow 1995). Since higher specific energy dissipation rates correlate with a greater potential for cell damage (Croughan et al. 1987; Nienow 2006), the down pumping impeller was chosen for the bioreactor culture. The choice of this impeller type and its relative size (D/T) fitted in well with an earlier study on microcarrier suspension (Ibrahim and Nienow 2004). The actual N_{JS} was 75 rpm for the bioreactor, whilst in the spinner flasks it was 30 rpm.

2.3 Analytical Techniques

A 1 mL sample was aseptically obtained from both the bioreactors and spinner flasks for analysis of pH, [glucose] mmol/L, [lactate] mmol/L, and [ammonium] mmol/L using a Nova Bioprofile FLEX bioanalyser (USA). Cell counting and viability (*via* propidium iodide exclusion) was done using a NucleoCounter NC-100 automatic

mammalian cell counter (Chemometec, Denmark). Samples for cell counting were determined whilst the cells were still attached to the microcarrier. Based on the viable cell number and metabolite data, the following parameters were determined:

1. Specific Growth Rate: $\mu = \frac{\left(Ln\left(Cx(t)/\,Cx(0)\right)\right)}{\Delta t}$

Where μ = specific growth rate (h^{-1}), *Cx(t)* and *Cx(0)* = cell numbers at the end and start of exponential growth phase respectively and t = time (h)

2. Doubling time: $t_d = \frac{Ln\,2}{\mu}$

Where t_d = doubling time (h) and μ = specific growth rate (h^{-1})

3. Fold Increase $= \frac{Cx(f)}{Cx(0)}$

where *Cx(f)* = maximum cell number and *Cx(0)* = initial cell number

4. Specific metabolite consumption rate: $q_{met} = \frac{\mu}{Cx(0)} \times \frac{C_{met\,(t)} - C_{met\,(0)}}{e^{\mu t} - 1}$

where q_{met} = specific metabolite consumption rate, μ = specific growth rate (h^{-1}), $C_{met(t)}$ and $C_{met(0)}$ = concentration of metabolite at the start and end of exponential growth phase respectively, *Cx(0)* = cell number at the start of exponential growth phase and t = time (h)

5. Lactate yield from glucose: $Y_{Lac/Glc} = \frac{\Delta[Lac]}{\Delta[Glc]}$

where $Y_{Lac/Glc}$ = lactate yield from glucose, Δ[Lac] = lactate production over specific time period and Δ[Glc] = glucose consumption over same time period

2.4 Harvesting

At day 8 of the culture, 60 mL was obtained from each bioreactor and placed into fresh 100 mL spinner flasks. The microcarriers were allowed to settle after which the medium was aspirated. The microcarriers were then washed with Ca^{2+} and Mg^{2+} free PBS and 60 mL trypsin (0.25%)/EDTA was added and spinner flasks were placed in a humidified CO_2 controlled incubator for 7 min. Whilst incubating and based on studies of particle abrasion (Nienow and Conti, 1978), the vessels were agitated briefly at 150 rpm to aid detachment. After incubation, the cells were quenched with 70 mL growth medium and vacuum filtered using a Steriflip® 60 µm filtration unit (Millipore, UK). The cell suspension was then centrifuged at 220 g for 5 min and resuspended in growth medium. Cell viability was determined using the NucleoCounter NC-100.

1.5 Cell characterisation

1.5.1 Immunophenotypic analysis

Immunophenotypic analysis of the hMSCs was determined by flow cytometry before expansion on the microcarriers and on the cells after harvesting. This was performed using a Beckman Coulter Quanta SC flow cytometer (Beckman Coulter, UK) with excitation at 488nm. Cells were prepared for analysis by centrifuging at 300 g. The supernatant was discarded and the cells were resuspended in flow cytometry stain buffer (R&D Systems, UK). A panel of mouse anti-human monoclonal antibodies was used to

target cell-surface receptors and was prepared in accordance with the manufacturer's instructions. The antibodies were based on the panel recommended by the ISCT (Dominici *et al.* 2006) and included CD73-PE, CD90-PE CD105-PerCP, CD14 FITC, CD19 FITC CD34-PE-Cy7 CD45-PE-Cy5, and HLA-DR-FITC (BD Biosciences, UK; R&D Systems, UK). Cells were incubated with the antibody in the dark at room temperature for 30 min. Associated isotype controls were also prepared for all experimental conditions. A minimum of 10 000 events were recorded for each sample and the data was analysed using FlowJo computer software (Treestar Inc, USA).

1.5.2 Differentiation capacity

The multi-lineage potential of the cells was ascertained by inducing the samples post-expansion with the StemPro Adipogenesis kit, StemPro Chondrogenesis kit and StemPro Osteogenesis kit (Life Technologies, UK). The differentiation media were prepared as per the manufacturer's instruction. Briefly, this involved thawing the supplement overnight and adding to the basal differentiation medium.

Chondrogenic differentiation involved the formation of a micromass of hMSCs, generated by seeding 5 µL of a cell suspension which was at a density of 1.6×10^7 cells.mL^{-1} into a microwell plate. The microwell plate was placed into the incubator for 2 h, after which 1 mL chondrogenic differentiation medium was added; the cells were then returned to the incubator. Cells undergoing adipogenic and osteogenic differentiation were seeded onto separate microwell plates at a cell density of 5000 cells.cm^2 in growth medium and left in a humidified incubator at 37 °C, 5 % CO_2 for 3 days. The growth medium was then replaced with either adipogenic or osteogenic

differentiation medium and returned to the incubator. The differentiation medium for each differentiation assay was replaced every 72 h until day 21, at which point the hMSCs undergoing osteogenesis were stained with alkaline phosphatase (ALP) and Von Kossa stains and those undergoing chondrogenic differentiation were stained with Alcian Blue.

For chondrogenic differentiation, after fixing the cells with 2% (v/v) paraformaldehyde (PFA) for 30 min at room temperature, cells were washed three times with Ca^{2+} and Mg^{2+} free PBS and 1% (w/v) Alcian Blue (chondrogenic) solution was added and incubated at room temperature for 60 min. Prior to observing under the microscope, the samples were washed with PBS three times and 1 mL distilled water was added. Upon final washing, the samples were observed under a Nikon TS-100 light microscope (Nikon, UK).

For osteogenic differentiation, the cells were fixed with 10% cold neutral-buffered formalin for 20 min at room temperature. Samples were then washed with Ca^{2+} and Mg^{2+} free PBS and kept in distilled water for 15 min at room temperature before incubating with 4% (v/v) Napthol AS-MX phosphate alkaline solution in a darkened at room temperature for 45 min. Prior to observing under a microscope, samples were washed three times with distilled water. Distilled water was then removed and samples incubated with 2.5% (v/v) silver nitrate solution for 30 min at room temperature. The samples were then washed with distilled water three times before observing under the Nikon light microscope.

1.5.3 *Plastic-adherence and cell morphology*

For plastic adherence and morphology cells obtained after harvesting were seeded into T-25 flasks to determine their ability to attach to tissue culture plastic as well as to qualitatively identify any morphological changes to the cells post-harvest. The cells were observed using the Nikon light microscope mentioned previously.

2. Results and Discussion

3.1 hMSC growth

The expansion of hMSCs on microcarriers in a stirred-tank bioreactor at the litre-scale was achieved over a period of 12 days. In parallel to the bioreactor study, hMSCs were also cultured in 100 ml spinner flasks at the same cell seeding density to surface area ratio. The microcarrier seeding density chosen, 6000 cells.cm^{-2}, equates to ~ 5 cells/bead. This was chosen based on preliminary work (Hewitt et al. 2011) and for comparability with standard T-flask culture where the seeding density used is typically 5000 cells.cm^{-2}. In all cases reproducible results were obtained (Figure 1 and Figure 2). In the 2 bioreactors, the maximum cell densities achieved were 1.68 x 10^5 cells/ml and 1.44 x 10^5 cells/ml by day 9. During this time, the dO_2, though not controlled, never fell below 45% of saturation, well above the level of 20% where previous work with these cells had shown a deterioration in performance ((Rafiq et al. 2013). Operating in this way and knowing the cell density as a function of time enabled an estimate of the specific oxygen uptake rate of the cells to be calculeated, the average value being ~ 8.1 fmol/cell h for bioreactor 1 and ~ 6.3 fmol/cell h for bioreactor 2.

The cell density achieved was similar to the maximum of 1.10 x 10^5 cells/ml and 1.50 x 10^5 cells/ml achieved in the 2 spinner flasks. However, it is notable that growth in the spinner flasks was slower than that in the bioreactors as the maximum cell densities in the latter were not reached until day 10. This is also reflected in the maximum specific growth rates and doubling times, 0.014 h^{-1} and ~ 80 h for the bioreactors and 0.006-0.013 h^{-1} and ~ 100-130 h for the spinner flasks respectively (Table 1). The doubling times are noticeably longer than those calculated for the same hMSCs in T-flask culture

which are typically 45-60 h depending on the medium exchange strategy used, if cultured at 37°C under conditions of 100% dO_2 (Rafiq et al. 2013; Schop et al. 2009)

Based on the maximum cell densities achieved, a greater than 6-fold expansion of the hMSCs in the bioreactors was realised, which is comparable to that from standard T-flask culture (ranging from 5-10 fold depending on the medium exchange strategy used, if cultured at 37°C under conditions of 100% dO_2 (Rafiq et al. 2013)). The number of cells obtained from the 5 L bioreactors is equivalent to 55 - 65 confluent T-175 tissue culture flasks (where confluence for a T-175 for this hMSC cell line is approximately 6.5 x 10^6 cells. A slightly lower fold expansion was achieved in both spinner flasks (3.66 and 5 for spinner flasks 1 and 2, respectively).

The metabolite profile for both the bioreactor and spinner flask cultures correlates well with the respective growth curves (Figures 1b and 2b), with increasing cell numbers resulting in a greater concentration of lactate and ammonium measured in the medium with a concomitant decrease in the concentration of glucose. The level of glucose decreases steadily during the initial stages in both culture systems and subsequently begins to decrease rapidly until cells reach their maximum cell densities (e.g. days 8 and 9 for the bioreactors) and reaches levels < 1 mmol/L. However immediately after a medium exchange, there is a measurable increase in the level of glucose and a decrease in the levels of lactate and ammonium as identified by the spikes at days 3, 5, 7, 9 and 11 (Figure 1b and 2b). In both culture systems, the level of lactate does not begin to increase until after day 6, where for example with the bioreactors, it rises from ~5.5 mmol/L, to ~ 10 mmol/L by day 11. Although similar trends are seen for both

bioreactors and spinner flasks, it is notable that in both spinner flasks, a higher lactate and ammonium concentration was measured at the end of the culture (~ 12 mmol/L lactate, 1.1 mmol/L ammonium) than for the bioreactors (~ 10 mmol/L lactate, 0.5 mmol/L ammonium). It is thought that this is not simply to do with differences in cell yields but probably due to a difference in the culture environments and this will be further explored below. However, in neither culture system do they reach growth inhibitory levels for hMSCs, which have been determined experimentally to be approximately > 20 mmol/L and > 2 mmol/L for lactate and ammonium respectively (Schop et al. 2009). Therefore, whilst the accumulation of these waste products can lead to detrimental effects on hMSC growth, it is more likely that glucose limitation was a major factor here. This suggestion is supported by the fact that glucose is considered the primary source for ATP through either oxidative phosphorylation (resulting in 30-38 moles of ATP for each molecule of glucose) or anaerobic glycolysis (resulting in 2 moles of ATP and 2 moles of lactate for each molecule of glucose). Thus, its presence is fundamental to cell proliferative capacity (Glacken 1988).

Analysis of the specific production and utilisation of lactate compared to glucose is interesting (Figure 3). In all cases, between days 9 and 12, the amount of lactate produced when compared to glucose consumed rises above 2 mol. mol^{-1}, which is the maximum theoretical yield of lactate from glucose (Glacken 1988). This observation suggests that another carbon source, most likely glutamine, is also being consumed which, when metabolised, degrades into lactate and ammonium (amongst other metabolites), hence resulting in higher lactate yields with a concomitant increase in ammonium concentration. The fact that this occurs earlier (day 9) for the bioreactors

than for the spinner flasks (day 10 – 11) reflects the shorter doubling time, maximum specific growth rates and higher fold increase in the former (Table 1).

Whilst the lack of glucose is one factor that is likely to impact cell expansion, it is also important to consider other factors. A significant advantage of culturing cells in a bioreactor system, as opposed to traditional monolayer culture in T-flasks or roller bottles, is the ability of online monitoring and control of various critical culture parameters, such as pH and dO_2. Whilst the dO_2 and pH were not directly controlled here, these parameters were monitored throughout the course of the bioreactor cultures (Figure 1c). The measurement of these parameters was not possible in the spinner flasks used in this work. As expected, there is a gradual decrease in both the pH and dO_2 as the culture conditions become more acidic as a result of lactate accumulation, and decrease in dO_2 as the cells consume oxygen. Previous work has demonstrated that with this cell line, there is a significant decrease in cell yield in monolayer culture conditions when grown under 20% dO_2 in comparison to 100% dO_2 (Rafiq et al. 2013) with an associated increase in both the glucose consumption and lactate production rates. After 12 days in culture the dO_2 for both bioreactors reaches approximately 50%. The decreasing oxygen levels in the medium may be a contributory factor in the inhibition of hMSC expansion as was found in the monolayer culture of this hMSC line under lower oxygen conditions (Rafiq et al. 2013). Likewise, the specific glucose consumption and lactate production rates (Figure 4) increase in both bioreactors towards the end of the culture (after day 9) when the oxygen level is lower, similar to the trend found previously in monolayer culture (Rafiq et al. 2013). It was thought that in the monoculture case that despite the lower cell number, the lower dO_2 levels caused the

cells to become quiescent (with respect to expansion), whilst still being metabolically active so as to adapt to the culture conditions. It is possible that this could also be occurring in the bioreactor when the oxygen level in the culture medium starts to decrease, resulting in an increase in the glucose consumption and lactate production rate towards the end of the culture, despite there being fewer cells.

As well as the oxygen concentration, pH is also a critical culture parameter. The pH in both bioreactors is initially ~7.2 but it steadily falls throughout the course of the culture to become increasingly acidic, reaching pH values of approximately 6.9 and 6.7 for bioreactors 1 and 2 respectively. This drop demonstrates that despite regularly refreshing the medium, which utilises a sodium biocarbonate buffer system, the culture conditions still become acidic as a result of lactic acid production and accumulation. This change results in a deviation from the physiological pH and therefore could also have an impact on cell growth.

In addition to the possibility that the medium culture conditions resulted in hMSC growth inhibition, another potential limiting factor is that of surface area. It was calculated that by day 9, the cells had achieved theoretical confluency of ~ 27 cells/microcarrier (based on equivalent monolayer culture confluence) and additional microcarriers were not added at any point during the culture. As a result, assuming confluence was achieved towards the end of the rapid growth phase, it is highly likely that this condition, in combination with the previously aforementioned factors (glucose limitations, decrease in pH and dO_2) resulted in the culture entering the stationary/death phase after day 9.

The fact that the growth at the 5 L scale, a larger scale than previously reported in the open literature, is somewhat better than in the spinner flask is clearly encouraging. It is interesting to consider whether this improvement can be explained by the different physical environment in the two cases. This difference is not only due to the potential for more precise measurement in the bioreactor, which showed that the dO_2 never fell close to the level (20%) at which a poorer performance had been observed in T-flasks ((Rafiq et al. 2013); and the fall in pH was not to an unacceptable level. It is also inherent in the different geometries and scales of the two. Firstly, in the spinner flask, the spinner is essentially a rather crude radial flow impeller whilst in the bioreactor, a down pumping axial flow impeller is used and it is well established that the latter require much less energy to suspend particles such as microcarriers (Ibrahim and Nienow 1996, 1999) In addition, the lack of baffles in the spinner flask compared to the bioreactor, even when the microcarriers are in motion, generally leads to a much less evenly distributed suspension with the particles concentrating in the lowest part of the flask (Nienow 1997a). Thus, it is possible that the poorer particle suspension characteristics of the spinner flask are impacting negatively on cell growth. Another important parameter that changes across the scales as well as with geometry is the quality of homogenisation. This parameter generally deteriorates on scale-up but it is also much poorer in the absence of baffles (Nienow 2006). This improved homogeneity due to baffling will become more important when pH is controlled by the addition of base and with increasing scale.

Thus, though at this stage it is not possible to give a precise explanation for the improvement from the spinner flasks to stirred bioreactor, the changes in these different parameters with geometrical configuration and scale are encouraging in relation to the

greater scale up that will be required for commercial production of cells for allogeneic thereapies (Want et al, 2012).

3.2 Cell Harvest

Whilst there is a clear need for the optimal attachment and proliferation of hMSCs, equally as important is the ability to successfully harvest hMSCs of sufficient quantity and quality. Using a novel and scalable harvesting strategy based on earlier literature on particle abrasion (Nienow and Conti 1978), cells were harvested from the microcarriers in 60 ml of the bioreactor culture (indeed we have now successfully scaled this up to 500 ml (data not shown)). By trypsinizing and agitating at a higher agitator speed in a separate vessel (for details refer to Section 2.4), the cells successfully detached from the microcarriers (Figure 5). Then, using the Steriflip® 60 µm filtration unit, the cells were filtered from the microcarriers and subsequently centrifuged. 60 ml samples were taken from each bioreactor after day 8 and after harvest, the total cell number from the 60 ml matched with the viable cells/ml value obtained via the day 8 sample based on the NucleoCount measurement, thereby validating the daily sampling and counting method.

3.3 Cell Quality

In order to determine the quality of the hMSCs and to identify whether there had been any change following microcarrier expansion in a bioreactor and the subsequent harvest, the cells were analysed according to the Dominici panel of markers (Dominici et al. 2006) to ascertain their immunophenotypic expression as well as tissue-culture adherence and morphology (both pre-inoculation and post-harvest) and for their multilineage differentiation potential.

For both bioreactors (Table 2), both pre-inoculation and post-harvest, >99% of the cell population were positive for CD73, CD90 and CD105, whilst for the negative markers CD14, CD19, CD34 and HLA-DR, <2% of the cell population was positive for these markers pre-inoculation, and this reduced even further to <1% post-harvest. Crucially, this set of data demonstrates that the immunophenotype of hMSCs are not affected by either the upstream or downstream processing, often a concern that cells will be sensitive to bioprocessing.

In all cases. hMSCs were able to adhere and grow on tissue culture plastic post-harvest whilst retaining their key morphological features, demonstrating similar morphology both before and after bioreactor culture (Figure 6). The multilineage differentiation potential of the cells was investigated post-harvest by inducing the hMSCs to differentiate towards the adipogenic, chondrogenic and osteogenic lineages. After 21 days in lineage-specific differentiation media, samples of all experimental conditions were found to be positive for alkaline phosphatase and von Kossa staining demonstrating osteogenic differentiation capability; positive for adipogenic differentiation through the clear formation of lipid vacuoles, and positive for Alcian Blue staining demonstrating chondrogenic differentiation capability (Figure 7). Therefore, the microcarrier bioreactor culture and subsequent harvest of hMSCs had no impact on the ability of the cells to retain their differentiation capacity. As such, the characterisation analyses have demonstrated that hMSCs have retained key quality attributes (identity and function – where function is linked to differentiation capacity) after large-scale bioprocessing.

3. Conclusions

The successful bioprocessing of human mesenchymal stem cells is not trivial. Indeed, expanding human stem cells in culture has been more of an art than a science, so much so that some laboratories do not grow human stem cells at all. Regenerative medicine promises to revolutionise clinical practise and the realisation of this promise requires the development of scalable growth and harvest strategies for the larger scale production of fully functional human stem cells. Here we report for the first time the successful growth of bone-marrow derived hMSCs in fully controllable 5 L bioreactors at a working volume of 2.5 L for a period of 12 days on plastic microcarriers. Moreover, a scalable harvesting strategy was developed to successfully detach a large volume of cells from the cell-microcarrier suspension, thus outlining the potential for the successful harvesting of large volumes of cells from microcarriers. Importantly, the bioprocessing unit operations had little effect, if any, on the quality of the cells for specific regenerative medicine purposes. It is believed that this is the first instance in which both the successful hMSC cell growth on microcarriers coupled with a detachment protocol from them for subsequent downstream processing at the litre scale has been reported in a peer-reviewed journal. However, it is recognised that the productivity of even the best bioreactor run, equivalent to that produced manually from 65 confluent T-175 flasks was insufficient to meet the demand for the high numbers of cells required for a single cell-based therapy. Nevertheless the results are promising given the opportunity for further optimisation of the culture conditions including feed strategy (e.g. perfusion) and the harvesting step as well as the advantage of scalability and online control with a fully instrumented bioreactor system. Importantly, the improved performance in the 5L baffled bioreactors compared to the spinner flasks is

particularly encouraging because such configurations are the easiest to scale-up (Nienow 2006), and there are physical studies of reactors and bioreactors in the literature to suggest that further increases in scale with such geometries are likely to be successful.

Acknowledgements

The authors would like to acknowledge the Biotechnology and Biological Sciences Research Council (BBSRC; UK) Bioprocessing Research Industries Club (BRIC), the Engineering and Physical Sciences Research Council (EPSRC; UK) and Lonza GmbH (Cologne, Germany) for their support and funding.

References

Croughan MS, Hamel JF, Wang DI (1987) Hydrodynamic effects on animal cells grown in microcarrier cultures. Biotechnol Bioeng 29 (1):130-141. doi:10.1002/bit.260290117

Dominici M, Le Blanc K, Mueller I, Slaper-Cortenbach I, Marini F, Krause D, Deans R, Keating A, Prockop D, Horwitz E (2006) Minimal criteria for defining multipotent mesenchymal stromal cells. The International Society for Cellular Therapy position statement. Cytotherapy 8 (4):315-317. doi:10.1080/14653240600855905

Dos Santos F, Andrade PZ, Abecasis MM, Gimble JM, Chase LG, Campbell AM, Boucher S, Vemuri MC, Silva CL, Cabral JM (2011) Toward a clinical-grade expansion of mesenchymal stem cells from human sources: a microcarrier-based culture system under xeno-free conditions. Tissue Eng Part C Methods 17 (12):1201-1210. doi:10.1089/ten.tec.2011.0255

Eibes G, dos Santos F, Andrade PZ, Boura JS, Abecasis MM, da Silva CL, Cabral JM (2010) Maximizing the ex vivo expansion of human mesenchymal stem cells using a microcarrier-based stirred culture system. J Biotechnol 146 (4):194-197. doi:10.1016/j.jbiotec.2010.02.015

Frauenschuh S, Reichmann E, Ibold Y, Goetz PM, Sittinger M, Ringe J (2007) A microcarrier-based cultivation system for expansion of primary mesenchymal stem cells. Biotechnol Prog 23 (1):187-193. doi:10.1021/bp060155w

Glacken MW (1988) Catabolic Control of Mammalian Cell Culture. Nat Biotech 6 (9):1041-1050

Hewitt CJ, Lee K, Nienow AW, Thomas RJ, Smith M, Thomas CR (2011) Expansion of human mesenchymal stem cells on microcarriers. Biotechnol Lett 33 (11):2325-2335. doi:10.1007/s10529-011-0695-4

Ibrahim S, Nienow AW (1995) Power curves and flow patterns for a range of impellers in newtonian fluids: $40 < Re < 5 \times 10^5$. Chem Eng Res Des 73 (5):485-491

Ibrahim S, Nienow AW (1996) Particle suspension in the turbulent regime : the effect of impeller type and impeller/vessel configuration. Chem Eng Res Des 74:679-688

Ibrahim S, Nienow AW (1999) Comparing impeller performance for solid suspension in the transitional flow regime with Newtonian fluids. Chem Eng Res Des 77:721-727

Ibrahim S, Nienow AW (2004) Suspenion of microcarriers for cell culture with axial flow impellers. Chem Eng Res Des 82:1082-1088

Jackson L, Jones DR, Scotting P, Sottile V (2007) Adult mesenchymal stem cells: differentiation potential and therapeutic applications. J Postgrad Med 53 (2):121-127

Nienow AW (1997a) The mixer as a reactor - liquid/solid systems. In: Harnby N, Edwards MF, Nienow AW (eds) Mixing in the process industries. 2nd edn. Butterworth Heinemann, London, pp 394-411

Nienow AW (1997b) The suspension of solid particles. In: Harnby N, Edwards MF, Nienow AW (eds) Mixing in the process industries. 2nd edn. Butterworth Heinemann, London, pp 364-393

Nienow AW (2006) Reactor engineering in large scale animal cell culture. Cytotechnology 50 (1-3):9-33. doi:10.1007/s10616-006-9005-8

Pittenger MF, Mackay AM, Beck SC, Jaiswal RK, Douglas R, Mosca JD, Moorman MA, Simonetti DW, Craig S, Marshak DR (1999) Multilineage Potential of Adult Human Mesenchymal Stem Cells. Science 284 (5411):143-147. doi:10.1126/science.284.5411.143

Rafiq QA, Coopman K, Nienow AW, Hewitt CJ (2013) A quantitative approach for understanding small-scale human mesenchymal stem cell culture - implications for large-scale bioprocess development. Biotechnol J. doi:10.1002/biot.201200197

Rowley J, Abraham E, Campbell A, Brandwein H, Oh S (2012) Meeting lot-size challenges of manufacturing adherent cells for therapy. Bioprocess International 10:16-22

Schop D, Janssen FW, Borgart E, de Bruijn JD, van Dijkhuizen-Radersma R (2008) Expansion of mesenchymal stem cells using a microcarrier-based cultivation system: growth and metabolism. J Tissue Eng Regen Med 2 (2-3):126-135. doi:10.1002/term.73

Schop D, Janssen FW, van Rijn LD, Fernandes H, Bloem RM, de Bruijn JD, van Dijkhuizen-Radersma R (2009) Growth, metabolism, and growth inhibitors of mesenchymal stem cells. Tissue Eng Part A 15 (8):1877-1886. doi:10.1089/ten.tea.2008.0345

Sun LY, Hsieh DK, Syu WS, Li YS, Chiu HT, Chiou TW (2010) Cell proliferation of human bone marrow mesenchymal stem cells on biodegradable microcarriers enhances in vitro differentiation potential. Cell Prolif 43 (5):445-456. doi:10.1111/j.1365-2184.2010.00694.x

Trounson A, Thakar R, Lomax G, Gibbons D (2011) Clinical trials for stem cell therapies. BMC Med 9 (1):52

van Wezel AL (1967) Growth of cell-strains and primary cells on micro-carriers in homogeneous culture. Nature 216 (5110):64-65

Want AJ, Nienow AW, Hewitt CJ, Coopman K (2012) Large-scale expansion and exploitation of pluripotent stem cells for regenerative medicine purposes: beyond the T flask. Regen Med 7 (1):71-84. doi:10.2217/rme.11.101

	Bioreactor 1	Bioreactor 2	Spinner flask 1	Spinner flask 2
Fold Increase	7.02	6.02	3.66	5.00
Doubling time (h)	76.8	83.4	128.0	103.4
Max specific growth rate (h^{-1})	0.014	0.014	0.006	0.013

Table 1 Fold increase, doubling time and maximum specific growth rate in each of the vessels

Table 2 Immunophenotypic expression of hMSCs before and after bioreactor culture

	Pre-inoculation (Day 0)	Post-bioreactor harvest (Day 13)
CD90 (+ve)	99.9 ± 0.1	99.7 ± 0.2
CD73 (+ve)	99.9 ± 0.0	99.9 ± 0.0
CD105 (+ve)	99.9 ± 0.1	99.9 ± 0.05
CD14 (-ve)	0.17 ± 0.01	0.35 ± 0.1
CD19 (-ve)	0.36 ± 0.004	0.79 ± 0.02
CD34 (-ve)	1.12 ± 0.15	0.1 ± 0.02
CD45 (-ve)	0.49 ± 0.03	1.71 ± 0.07
HLA-DR (-ve)	0.49 ± 0.05	0.962 ± 0.04

Figure 1: The growth of hMSCs in 5 L bioreactor vessels over 12 days. A) Viable cells/ml readings for bioreactor 1 (left) and bioreactor 2 (right), B) nutrient and metabolite concentrations for bioreactor 1 (left) and bioreactor 2 (right), C) pH and dO_2 readings for bioreactor 1 (left) and bioreactor 2 (right).

Figure 2: The growth of hMSCs in 100 ml spinner flasks over 12 days. A) Viable cells/ml readings for spinner flask 1 (left) and spinner flask 2 (right), B) nutrient and metabolite concentrations for spinner flask 1 (left) and spinner flask 2 (right).

Figure 3: Yields of lactate from glucose for each vessel with readings from days 9 to 12. Reference point at 2 mol mol^{-1} as this is the maximum theoretical yield of lactate from glucose.

Figure 4: Specific growth, glucose consumption and lactate production rates for bioreactor 1 (A) and bioreactor 2 (B) over 12 days.

Figure 5: Images of hMSCs which have been successfully detached from the microcarrier surface after harvesting. A) Plastic P102-L microcarrier bead, B) harvested hMSCs.

Figure 6: hMSC morphology when cultured on tissue culture plastic before inoculation (left) and after harvesting (right).

Figure 7: Differentiation potential of hMSCs after harvesting down the adipogenic (left), osteogenic (centre) and chondrogenic (right) lineages.

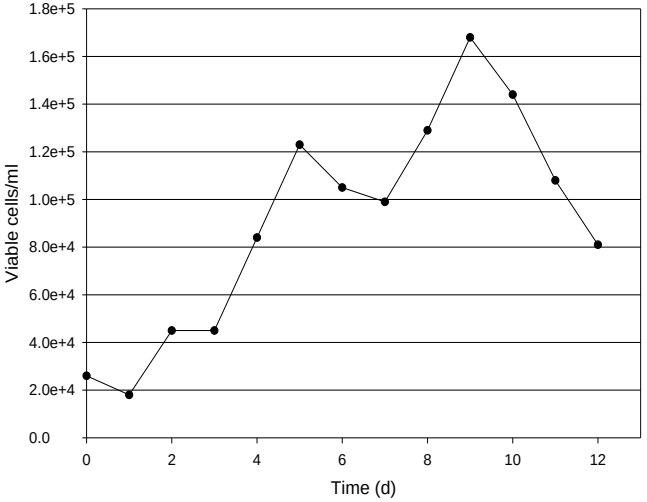
Viable cells/ml
1.8e+5
1.6e+5
1.4e+5
1.2e+5
1.0e+5
8.0e+4
6.0e+4
4.0e+4
2.0e+4
0.0
0
2
4
6
8
10
12
Time (d)

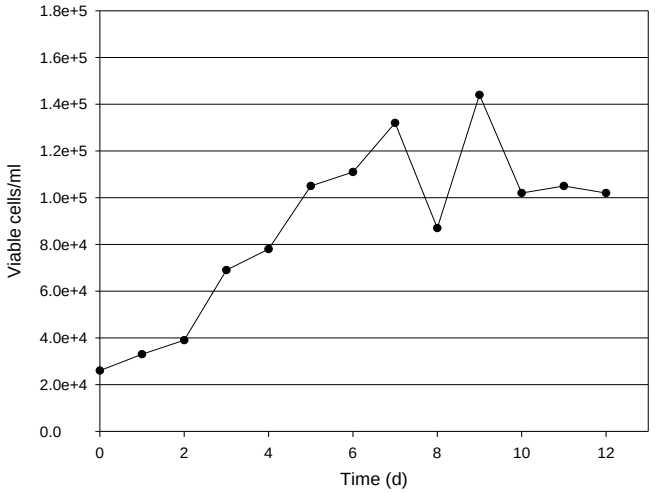
Viable cells/ml
1.8e+5
1.6e+5
1.4e+5
1.2e+5
1.0e+5
8.0e+4
6.0e+4
4.0e+4
2.0e+4
0.0
0
2
4
6
8
10
12
Time (d)

A

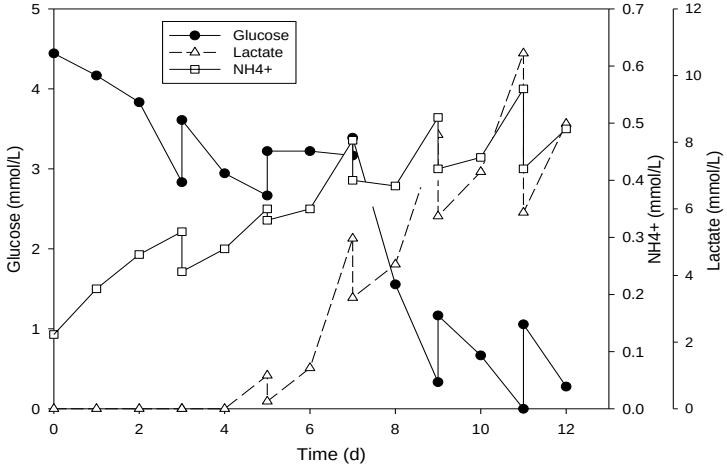
Glucose
Lactate
NH4+
Glucose (mmol/L)
NH4+ (mmol/L)
Lactate (mmol/L)
0
1
2
3
4
5
0.0
0.1
0.2
0.3
0.4
0.5
0.6
0.7
0
2
4
6
8
10
12
0
2
4
6
8
10
12
Time (d)

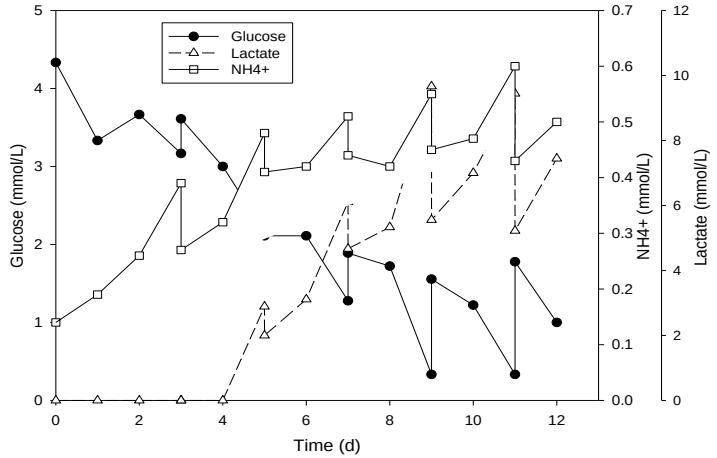
Glucose
Lactate
NH4+
Glucose (mmol/L)
NH4+ (mmol/L)
Lactate (mmol/L)
0
1
2
3
4
5
0.0
0.1
0.2
0.3
0.4
0.5
0.6
0.7
0
2
4
6
8
10
12
0
2
4
6
8
10
12
Time (d)

B

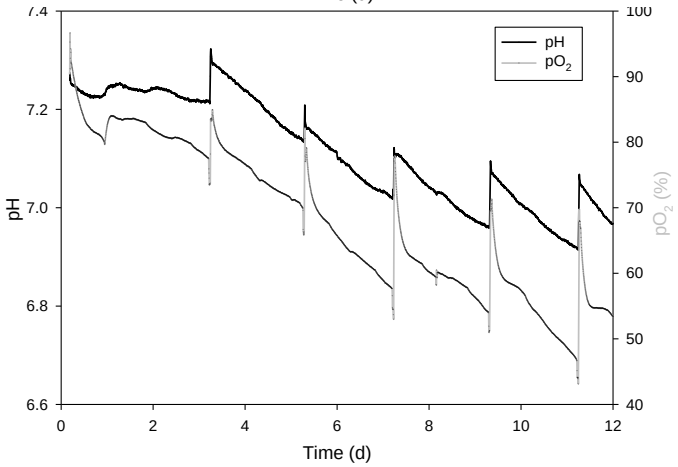
pH
pO2
pH
pO2 (%)
6.6
6.8
7.0
7.2
7.4
40
50
60
70
80
90
100
0
2
4
6
8
10
12
Time (d)

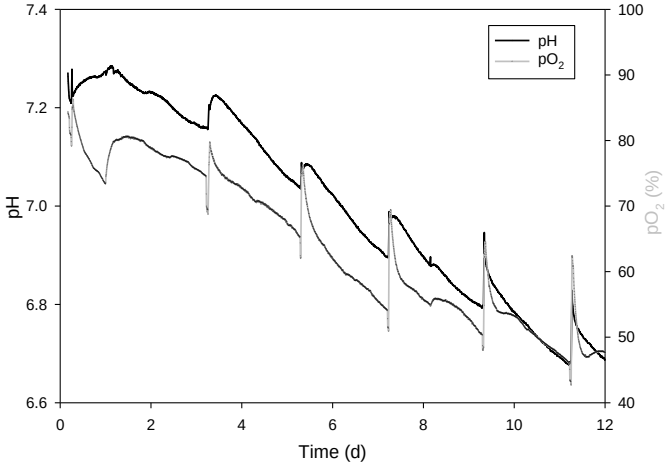
pH
pO2
pH
pO2 (%)
6.6
6.8
7.0
7.2
7.4
40
50
60
70
80
90
100
0
2
4
6
8
10
12
Time (d)

C

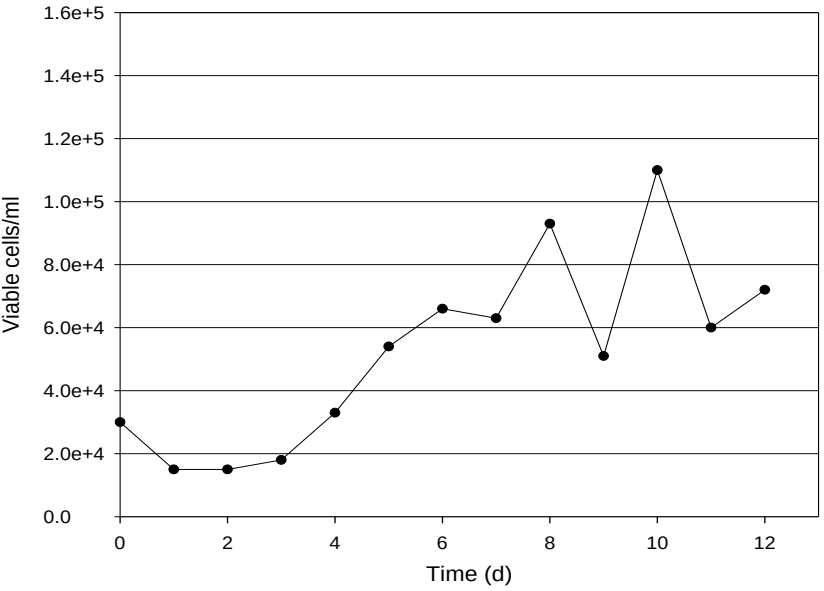
Viable cells/ml
1.6e+5
1.4e+5
1.2e+5
1.0e+5
8.0e+4
6.0e+4
4.0e+4
2.0e+4
0.0
0
2
4
6
8
10
12
Time (d)

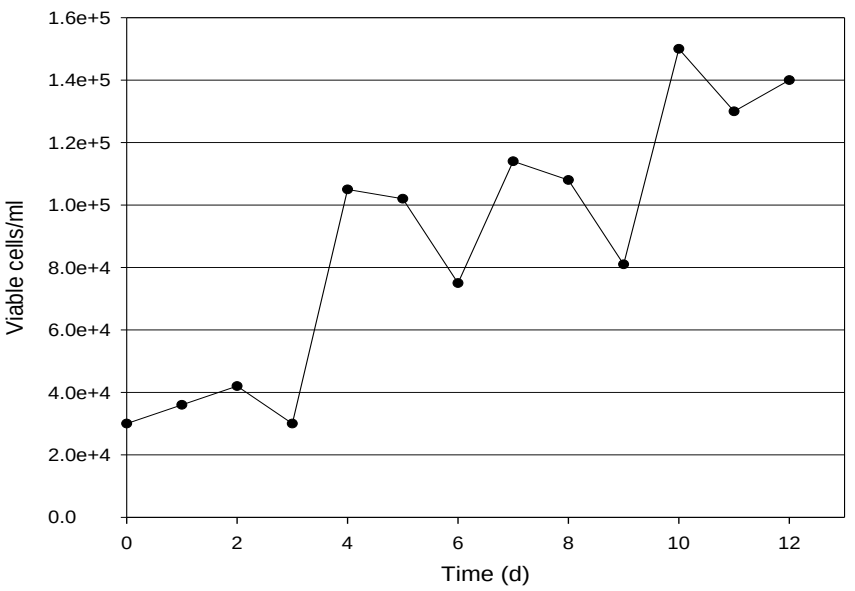
Viable cells/ml
1.6e+5
1.4e+5
1.2e+5
1.0e+5
8.0e+4
6.0e+4
4.0e+4
2.0e+4
0.0
0
2
4
6
8
10
12
Time (d)

A

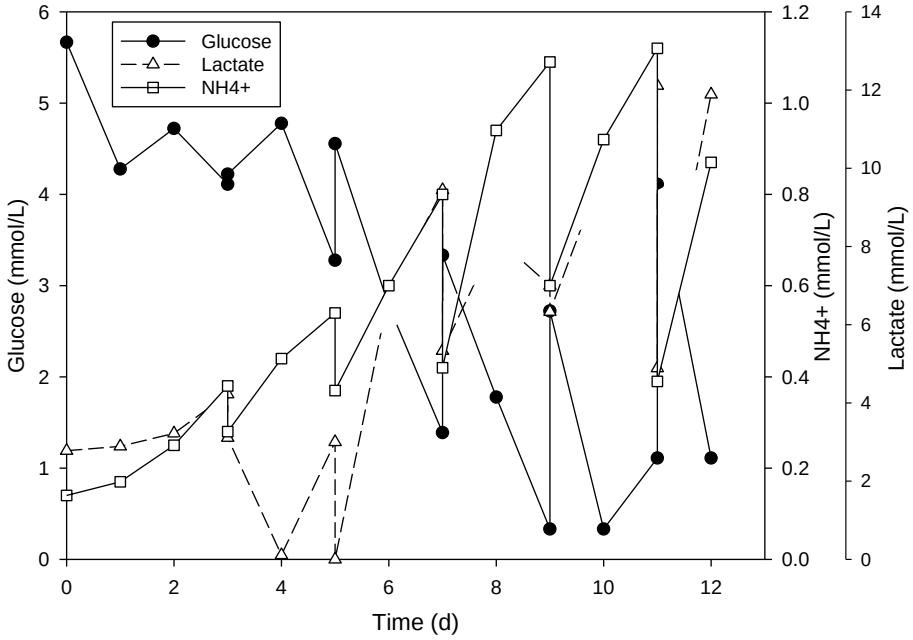
Glucose
Lactate
NH4+
Glucose (mmol/L)
NH4+ (mmol/L)
Lactate (mmol/L)
0
1
2
3
4
5
6
0.0
0.2
0.4
0.6
0.8
1.0
1.2
0
2
4
6
8
10
12
14
0
2
4
6
8
10
12
Time (d)

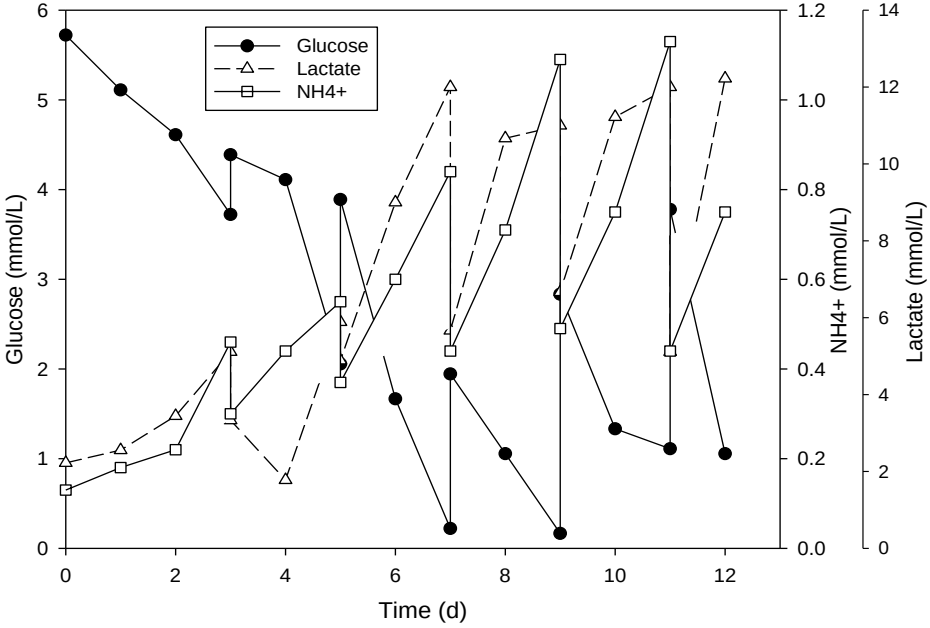
Glucose
Lactate
NH4+
Glucose (mmol/L)
NH4+ (mmol/L)
Lactate (mmol/L)
0
1
2
3
4
5
6
0.0
0.2
0.4
0.6
0.8
1.0
1.2
0
2
4
6
8
10
12
14
0
2
4
6
8
10
12
Time (d)

B

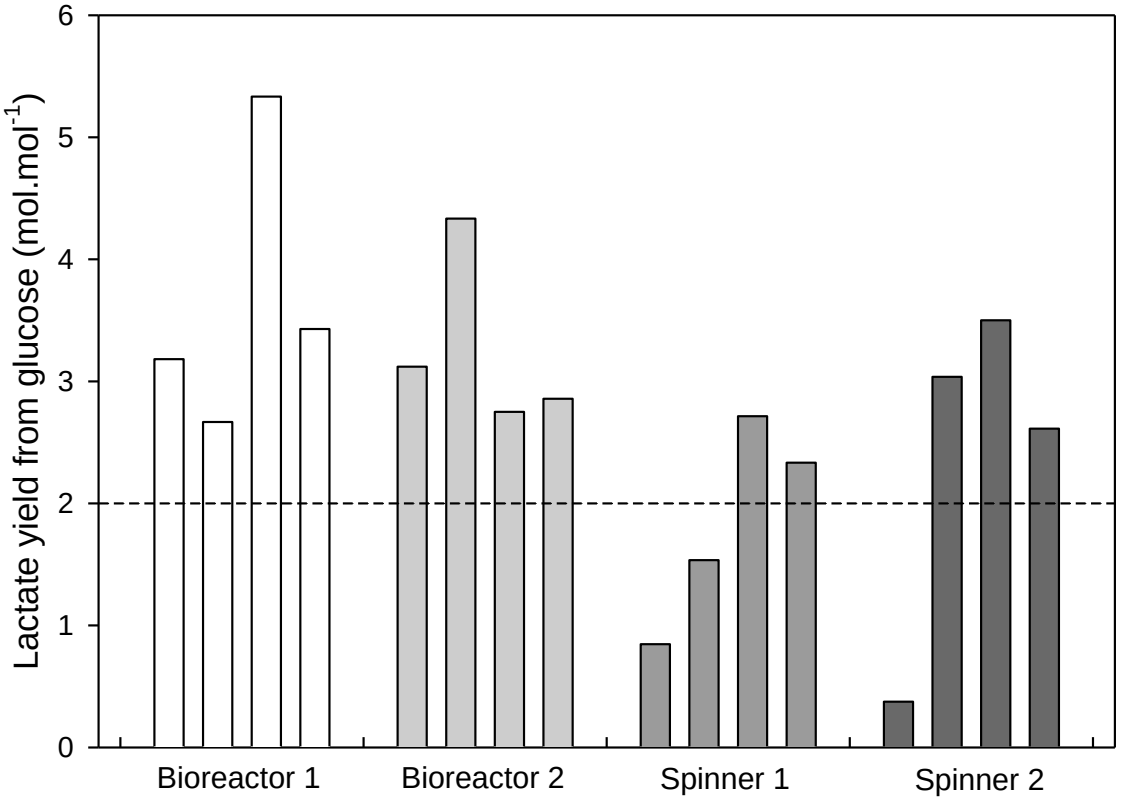
Lactate yield from glucose (mol.mol-1)
6
5
4
3
2
1
0
Bioreactor 1
Bioreactor 2
Spinner 1
Spinner 2

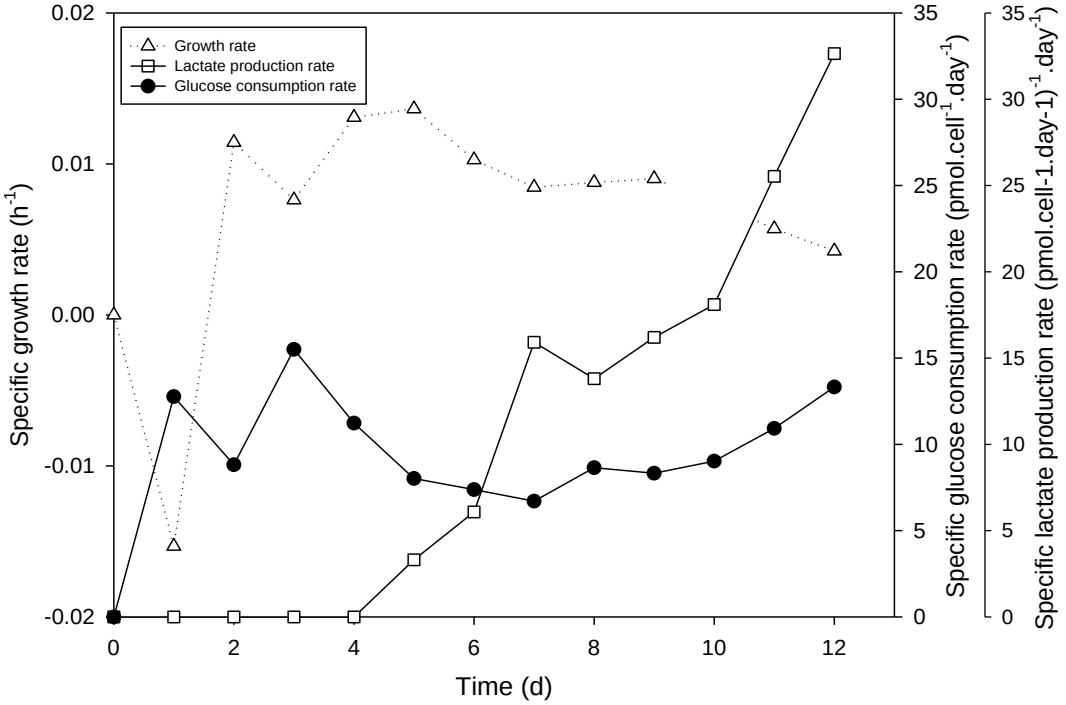
Growth rate
Lactate production rate
Glucose consumption rate
Specific growth rate (h-1)
Specific glucose consumption rate (pmol.cell-1.day-1)
Specific lactate production rate (pmol.cell-1.day-1)-1.day-1)
Time (d)
0.02
0.01
0.00
-0.01
-0.02
0
2
4
6
8
10
12
35
30
25
20
15
10
5
0

A

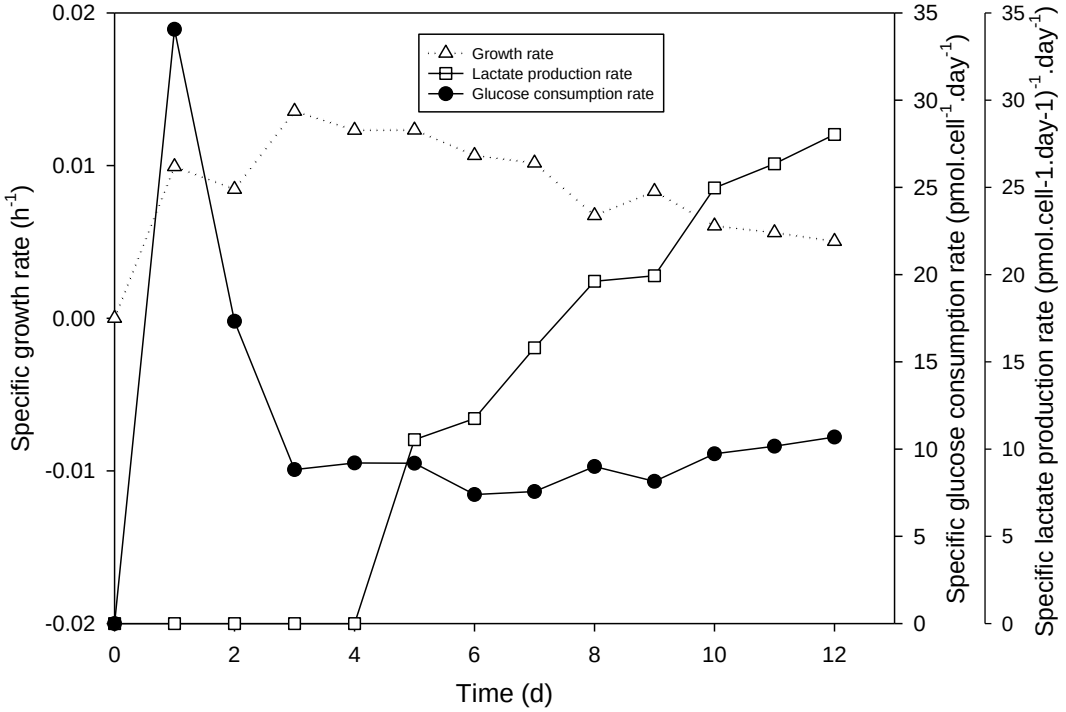
Growth rate
Lactate production rate
Glucose consumption rate
Specific growth rate (h-1)
Specific glucose consumption rate (pmol.cell-1.day-1)
Specific lactate production rate (pmol.cell-1.day-1)-1.day-1)
Time (d)
0.02
0.01
0.00
-0.01
-0.02
0
2
4
6
8
10
12
35
30
25
20
15
10
5
0

B

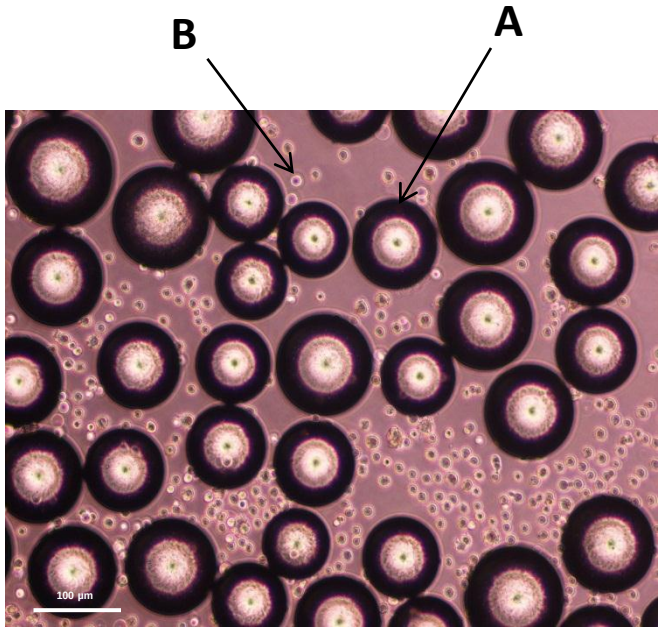
B
A
100 µm

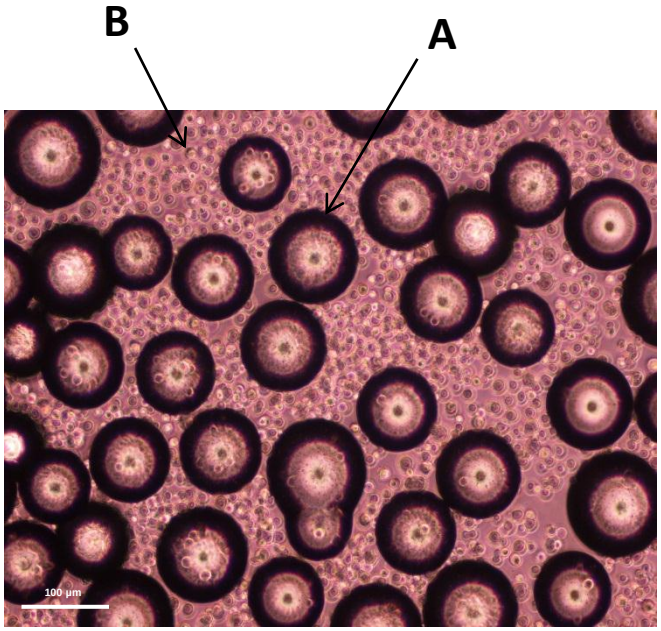
B
A
100 µm

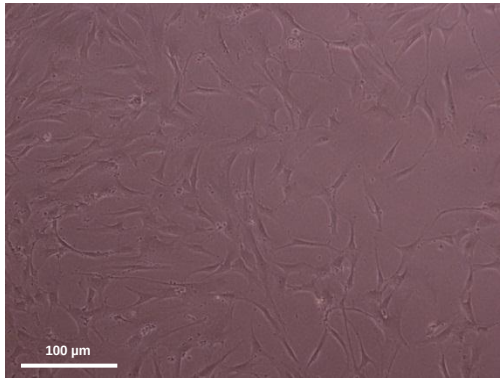

(pre-inoculation)

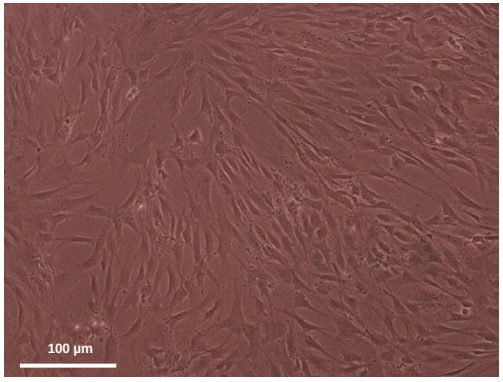

(post-harvest)

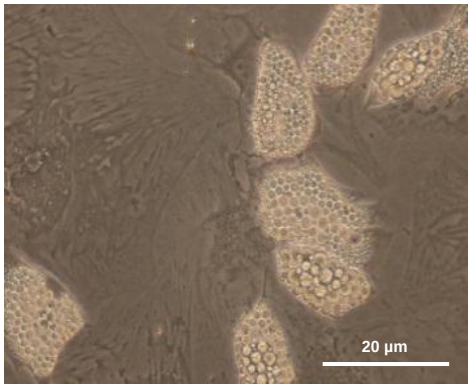

Adipogenic

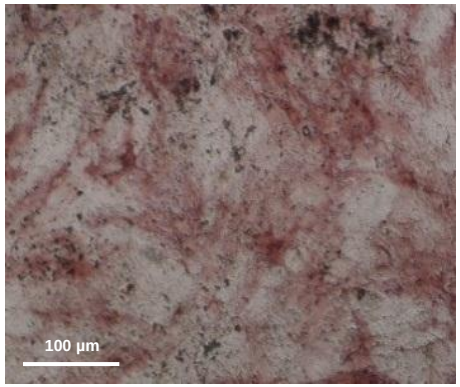

Osteogenic

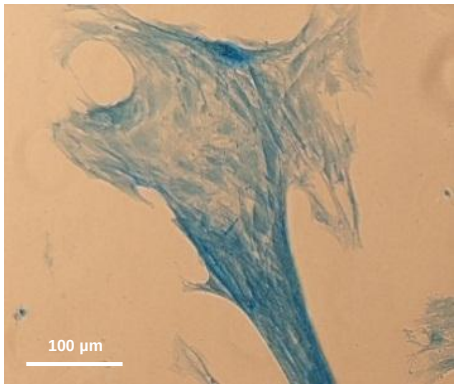

Chondrogenic